STANFORD MECHANICAL ENGINEERING

Emissions Control in Swirl-Stabilized Combustors

A collaborative program including:
The University of Cincinnati
The Naval Research Laboratory
Stanford University

Sponsored by the Office of Naval Research: N00014-02-1-0837

Final Report for the Stanford University Task:

University of Cincinnati subcontract: OSP 03102

Optical Sensors for Combustion

Stanford University PI: Professor Ronald K. Hanson
High Temperature Gasdynamics Laboratory
Department of Mechanical Engineering
Stanford University, Stanford, CA 94305
650-723-6850
rkhanson@stanford.edu

Period of performance:
July 12, 2002 thru July 14, 2006

December 2006

Table of Contents

EXECUTIVE SUMMARY

The Stanford University portion of this collaborative project has four major goals: 1) develop real-time tunable-diode-laser (TDL)-based sensors for combustion control, 2) demonstrate the use of these sensors to measure temperature in liquid-fueled swirl-stabilized flames at the University of Cincinnati, 3) fabricate a swirl-stabilized gas and liquid fuel burner with optical access to enable diagnostic development that mimics the atmospheric pressure performance of the University of Cincinnati facility, and 4) demonstrate the use of the TDL sensor for combustion control in this burner.

Early in the project, we designed, fabricated, and tested a first generation TDL temperature sensor using water vapor absorption near 1.8μm. After testing the sensor in well-controlled heated-cell and in stable laminar flames at Stanford University, this first generation temperature sensor was used for measurements a practical swirl-stabilized burner at the University of Cincinnati. The ±20K accuracy at 500Hz illustrated the potential for TDL laser temperature sensing for combustion control. The time-resolved (500Hz) measurements of gas temperature obtained were the first use of TDL temperature sensing in a liquid-fueled combustor. These measurements also demonstrated the ability to monitor temperature fluctuations in a forced flame and illustrated the potential to identify of combustion instabilities using a fast Fourier transform (FFT) of time-resolved temperature measurements.

Based on the success of this first measurement campaign, a second-generation, fiber-coupled, real-time temperature sensor near 1.4μm was designed, fabricated, and tested at Stanford University. This new design incorporated scanned-wavelength-modulated spectroscopy (scanned WMS) with second harmonic detection (*2f*) to enable

realtime temperature with a 2kHz bandwidth. Static cell measurements validated the accuracy of this new temperature sensor, the hardware and software for real-time data acquisition and analysis were developed, and real-time thermometry was demonstrated in a laboratory flame at 2kHz. The potential for combustor control using this new sensor was demonstrated on a second measurement campaign at the University of Cincinnati.

The University of Cincinnati swirl-stabilized burner concept using a GE-Goodrich TAR fuel injector was constructed at Stanford University with the optical access needed for characterization of the flame with wide range of optical diagnostics tools. Control of forced flame instabilities and the suppression lean-blow-out (LBO) were demonstrated using the second-generation, scanned WMS-2f TDL temperature sensor in the Stanford burner facility. Low-frequency fluctuations of the flame at fuel/air equivalence ratios just greater than LBO were detected by the temperature sensor. These fluctuations were identified in the time-resolved temperature measurements and provided an excellent precursor to incipient LBO. The strength of the temperature fluctuations were used as a control variable to successfully suppress LBO. These experiments are the first demonstration of LBO suppression with a physics-based heat-release control variable.

TECHNICAL ACCOMPLISHMENTS

I. Introduction

Tunable diode laser (TDL) sensors are useful diagnostic tools for propulsion and combustion applications providing time-resolved measurements of gas temperature, species concentration, gas velocity, as well as mass and momentum flux.[1] Water vapor (H_2O) is an ideal species to monitor because it is naturally present in air, is one of the primary products of hydrocarbon combustion, and absorbs strongly throughout the near-infrared region. Two-line thermometry based on high-resolution-absorption spectroscopy of H_2O has been developed and demonstrated in variety of reactive environments. For example, Furlong *et al.* [2] successfully demonstrated a multiplexed TDL sensor using two H_2O transitions near 1.34 μm and 1.39 μm for combustion control of an acoustically-forced dump-combustor; Ebert *et al.*[3,4] measured gas temperature in large scale gas- and coal-fired combustion systems using water transitions near 812 nm; Sanders *et al.*[5] measured gas temperature in pulse detonation engines using water transitions near 1.4μm, and Rieker *et al.*[6] and Mattison *et al.*[7] used similar transitions for temperature during the compression stroke of an IC engine. Lastly, Liu *et al.*[8] developed an applied scanned-wavelength direct absorption of water vapor near 1.4μm to monitor temperature at kHz rates in a model scramjet combustor.

However, these previous TDL temperature sensors used a wavelength-multiplexing scheme requiring multiple lasers. If transitions can be selected close enough together to be covered with the few cm^{-1} scan range of a typical TDL, the complexity of the wavelength-multiplexed scheme can be avoided. A few single-laser TDL temperature sensors have been reported previously, based on fortuitous coincidences of diode laser

wavelengths and water transitions; for example, Arroyo *et al.*[9] identified a useful H_2O line pair near 1.38 μm for single-laser H_2O thermometry, and more recently, Gharavi *et al.*[10] investigated a H_2O line pair near 1.48 μm for temperature measurements. In our recent work, we have utilized a design-rule based strategy to systematically evaluate and optimize the selection of H_2O vapor transitions from the vast number of possibilities in the region1-2 μm[11-13]. This work has led to the development on this project of two single-TDL temperature sensors, one using direct absorption near 1.8 μm[11] and the other using scanned-wavelength-modulation spectroscopy with second harmonic detection (scanned-WMS-2f) near 1.4 μm.[12] For each of these sensors, the logic of the line selection process was examined, the fundamental spectroscopic data for the selected lines was carefully measured in a heated cell, and the sensor performance was validated in a controlled laboratory environment.[11,12]

Here we summarize this work with a systematic comparison of the performance of Stanford's direct absorption temperature sensor near 1.8μm and the scanned-WMS-2f temperature sensor near 1.4μm, using measurements in a swirl-stabilized, atmospheric-pressure combustor at the University of Cincinnati; a preliminary report of these measurements was presented at the AIAA's Aerospace Sciences Meeting in 2005.[14] To our knowledge this work presents the first TDL thermometry in a liquid-fueled, swirl-stabilized spray flame. The performance differences between the scanned-WMS-2f and wavelength-scanned direct absorption are discussed in detail. The use of line selection to minimize ambient interference is illustrated. The measurements demonstrate the ability of TDL temperature sensing to monitor temperature fluctuations in harsh, practical

environments, and thus illustrate the potential of TDL sensors to provide a temperature-based control variable.

The second-generation scanned WMS-2f 1.4μm temperature sensor was used to control forced instabilities in an atmospheric pressure swirl-stabilized flame at Stanford. The sensor was then used to develop a physics-based control variable (based on temperature along a selected line-of-sight) and used to demonstrate the suppression of lean blow-out.

II. Absorption Spectroscopy Fundamentals

The sensor design and operation of the 1.8 μm time-resolved and the 1.4 μm real-time temperature sensors are detailed in refs. 11 and 12, respectively. We present here only the design information needed to compare direct-absorption and WMS-2f sensor strategies.

A. Direct absorption temperature sensor

The fractional transmission (τ_ν) of monochromatic laser light at frequency ν along a uniform path is described by the Beer-Lambert relation:

$$\tau_\nu = \left(\frac{I(\nu)}{I_o(\nu)}\right) = \exp\left(-P \cdot X_i \cdot S(T,\nu_j) \cdot \phi_\nu \cdot L\right) = \exp(-\alpha_\nu) \qquad (1)$$

where $I(\nu)$ and $I_0(\nu)$ are the transmitted and incident intensities, P [atm] is the total pressure, X_i is the mole fraction of the absorbing (i^{th}) species, $S(T, \nu_j)$ [$cm^{-2}atm^{-1}$] is the line strength of the j^{th} transition centered at ν_j [cm^{-1}], ϕ_ν [cm] is the line-shape function of the particular transition probed, which is normalized such that $\int\phi(\nu)d\nu \equiv 1$, and L [cm] is the path length. The combined quantity $\alpha_\nu = P \cdot X_i \cdot S(T,\nu_j) \cdot \phi_\nu \cdot L$ is known as the absorbance, and the integrated absorbance for the j^{th} transition is $A_j \equiv \int\alpha_\nu d\nu$.

The temperature can be inferred from the measured ratio of integrated absorbance for two different temperature-dependent transitions (illustrated in Fig. 1). Because the two integrated absorbances are obtained with the same partial pressure of water and same path length, the ratio of these two integrals reduces simply to the ratio of line strengths:

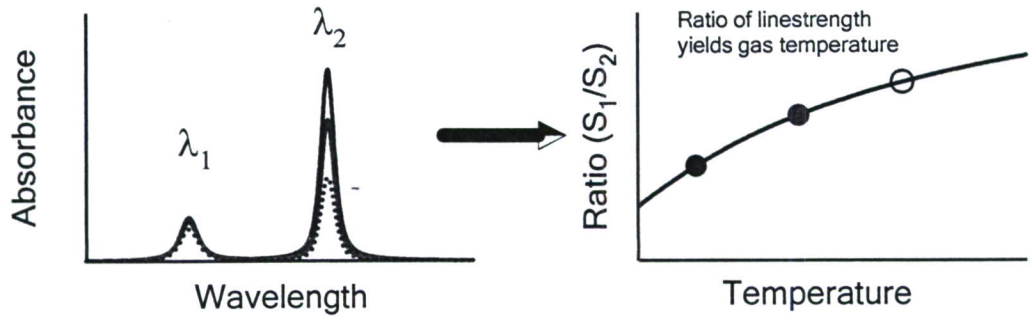

Fig. 1. Illustration of the measurement principle of the wavelength-scanned direct absorption 1.8 μm sensor: temperature inferred from the ratio of integrated absorbance of two different temperature-dependent transitions

$$R = \frac{A_1}{A_2} = \frac{\int PX_i S_1(T,\nu_1)\phi_\nu L d\nu}{\int PX_i S_2(T,\nu_2)\phi_\nu L d\nu} = \frac{S_1(T,\nu_1)}{S_2(T,\nu_2)} = \frac{S(T_o,\nu_1)}{S(T_o,\nu_2)} \exp\left[-\left(\frac{hc}{k}\right)\left(E_1'' - E_2''\right)\left(\frac{1}{T} - \frac{1}{T_o}\right)\right] \quad (2)$$

where the reference temperature is T_0 [K], E_j" is the lower state energy of the j^{th} transition [cm^{-1}], and T is the gas temperature (K).

B. Scanned WMS-2f temperature sensor

For scanned-wavelength modulation absorption spectroscopy, the laser is driven by a combination of slow ramp and a fast sinusoidal modulation, and the laser output frequency can be expressed by:

$$\nu(t) = \overline{\nu(t)} + a\cos(2\pi ft) \quad (3)$$

where $\overline{\nu(t)}$ [cm^{-1}] is the center frequency of the modulation and varies slowly in time, a [cm^{-1}] is the modulation amplitude and f [Hz] is the modulation frequency. Following refs. 15-18, the quantity τ can be expanded in a Fourier cosine series:

$$\tau\left[\overline{\nu(t)} + a\cos(2\pi ft)\right] = \sum_{n=0}^{+\infty} H_n\left[\overline{\nu(t)}, a\right]\cos(2\pi nft) \quad (4)$$

where $H_n[\overline{\nu(t)}, a]$ is the nth Fourier coefficient of the transmission coefficient[16]

$$H_o[\overline{\nu(t)}, a] = \frac{1}{2\pi}\int_{-\pi}^{\pi}\tau[\overline{\nu(t)} + a\cos\theta]d\theta \tag{5}$$

$$H_n[\overline{\nu(t)}, a] = \frac{1}{\pi}\int_{-\pi}^{\pi}\tau[\overline{\nu(t)} + a\cos\theta]\cdot\cos(n\theta)d\theta \tag{6}$$

Typically the second harmonic component of the signal is detected, and in the limit of weak absorbance (<0.1), this Fourier coefficient is given by

$$H_2[\overline{\nu(t)}, a] = -\frac{S\cdot P\cdot X_i\cdot L}{\pi}\int_{-\pi}^{\pi}\phi[\overline{\nu(t)} + a\cos\theta]\cdot\cos(2\theta)d\theta$$

The 2f signal is proportional to $I_0 H_2(\overline{\nu}, a)$ if intensity modulation effects are neglected.[16]

Similar to direct absorption technique, WMS-2f employs the two-line method for temperature measurements, as the 2f peak height ratio of two transitions is a function of temperature (Fig. 2), closely related to the ratio of the absorption line strengths.[17]

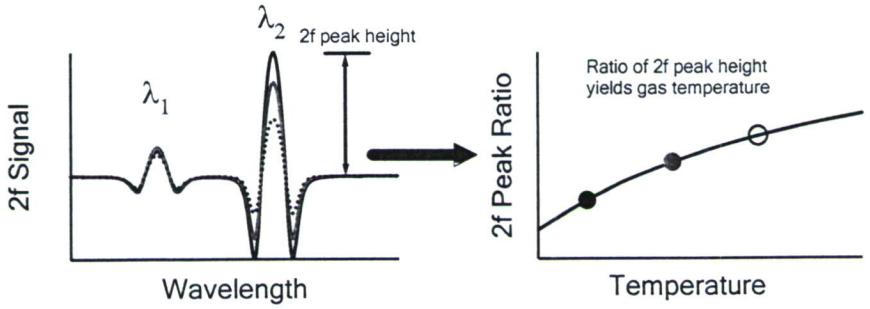

Fig. 2 Illustration of the measurement principle of the 1.4 μm sensor: temperature inferred from 2f peak ratio of two different temperature-dependent transitions

$$R_{2f,ratio} = \frac{I_{\overline{\nu_1}}}{I_{\overline{\nu_2}}}\cdot\frac{H_2(\overline{\nu_1})}{H_2(\overline{\nu_2})} = \frac{I_{\overline{\nu_1}}}{I_{\overline{\nu_2}}}\cdot\frac{S_1(T)}{S_2(T)}\cdot\frac{\int_{-\pi}^{\pi}\phi[\overline{\nu_1} + a_1\cos\theta]\cos(2\theta)d\theta}{\int_{-\pi}^{\pi}\phi[\nu_2 + a_2\cos\theta]\cos(2\theta)d\theta} \tag{8}$$

where $I_{\overline{\nu_1}}$ and $I_{\overline{\nu_2}}$ are the laser intensities at line center of transitions 1 and 2, respectively, and $H_2(\overline{\nu_1})$ and $H_2(\overline{\nu_2})$ are the second harmonic Fourier coefficients which are given by Eq. (7).

C. Comparison of 1.8 μm direct absorption and 1.4 μm WMS-2f temperature sensors

The calculated spectroscopic features for the water line pairs of the 1.4 μm and the 1.8 μm sensors are shown in Fig. 3 for temperatures of 296, 1000, and 2000K, and the transitions are listed in Table 1. The line selection of these two sensors and the quantitative spectroscopy of the target lines and their neighbors has been discussed in detail.[11,12] Both sensors use the two-line concept although there are additional

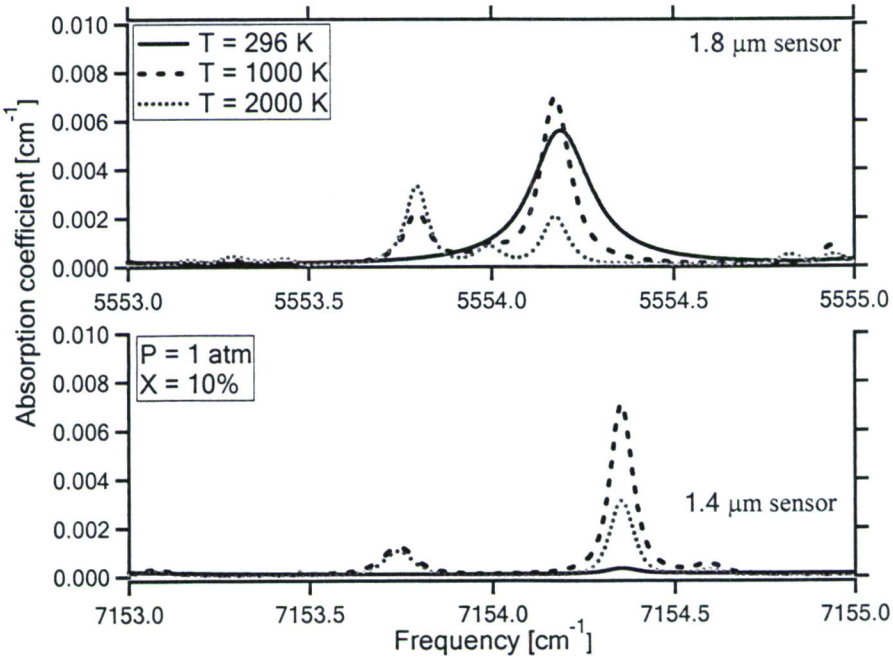

Fig. 3. Calculated spectroscopic features for water line pairs in the 1.4 μm and 1.8 μm sensors based on HITRAN[19]; X_{H2O} = 10%.

Table 1. Spectroscopic data for the 1.4 μm and 1.8 μm temperature sensor.

Line #	Frequency [cm^{-1}]	Line strength @ 296 K [cm^{-2}/atm]	Lower state energy [cm^{-1}]
1.8μm Sensor			
2 (high E")	5553.86	7.30×10^{-7}	3314.9
3	5554.04	3.63×10^{-7}	3139.5
1 (low E")	5554.18	7.66×10^{-3}	982.9
4	5554.21	9.20×10^{-3}	173.4
1.4μm Sensor			
High E" 1	7153.72	1.90×10^{-6}	2552.9
High E" 2	7153.75	6.15×10^{-6}	2552.9
Low E"	7154.35	3.67×10^{-4}	1789.0

neighboring transitions, and the 1.8 μm scan includes four lines while the 1.4 μm scan includes three. For the 1.8 μm case, the target lines 1 and 2 are resolved from line 3, and line 4 has negligible absorbance for temperatures above 800K (the lower bound temperature for this sensor; note that at lower temperatures the absorbance of the high E" transition becomes too weak for a precise ratio with the absorbance of the low E" transition). For the 1.4 μm case, the two high E" lines are completely blended at atmospheric pressure and are considered as a single line with the total linestrength the sum of the two contributions.

The 1.8 μm line pair is more sensitive to temperature while the 1.4 μm line pair is less sensitive to interference from ambient water vapor. The lower state energy difference (Δ E") of the 1.8 μm line pair is 2332 cm^{-1}, and the Δ E" of the 1.4 μm line pair is 764 cm^{-1}. Because the temperature sensitivity is highest for the largest difference[11,12] in $\Delta E'' = \left| E_1'' - E_2'' \right|$, the temperature sensitivity of the 1.8 μm sensor is about 3 times better than the 1.4 μm sensor. Because the laser scan of the 1.8μm sensor

has two low-energy transitions (E"~983cm^{-1} and E"~173cm^{-1}), the 1.8 μm sensor is sensitive to interference from ambient water vapor, as seen in Fig. 3 by the relatively large absorbance at 296K. Thus, this sensor requires the use of nitrogen or dry air to purge the laser path outside the measurement zone to eliminate interference ambient humidity in the air. Because the lowest energy transition in the scan of the 1.4 μm sensor has an E" near 1789 cm^{-1}, this sensor is insensitive to interference from cold humid room air as illustrated in Fig. 3 by the relatively small absorption observed at 296K.

Data analysis of injection-current tuned TDL direct absorption requires baseline fitting to account for the change in laser intensity as the laser frequency is tuned. Because the absorption signal is a small change in the transmitted intensity, the integrated absorbance is more precisely determined by the use of a Voigt fit to the lineshape. This analysis is time consuming and requires post-processing for rapid (kHz) time resolution. By contrast, the near-zero baseline of the WMS-2f signal and its significantly larger signal-to-noise ratio (SNR), compared to direct absorption measurements of small (less than a few %) absorbance, enables use of the ratio of the 2f peak heights to infer temperature. This avoids time-consuming fits and enables realtime data analysis of the temperature fluctuations with the scanned WMS-2f sensor. In these experiments, we demonstrated a 2 kHz measurement rate with this approach.[12]

For practical combustor applications, the use of fiber-coupled lasers and fiber components simplifies the implementation of the TDL sensor. Such fiber technology is well developed in the telecommunications wavelength region (1.3-1.65μm) and thus the sensor at 1.4 μm has many attractive features that are superior to the free-space lasers and optics at 1.8 μm. These include advanced laser performance, simple installation, easy

laser beam alignment, improved ruggedness and flexibility, and reduced overall system cost.

III. Combustion Measurements

Stanford's 1.4 μm and 1.8 μm TDL sensors were used for temperature measurements in an atmospheric-pressure swirl-stabilized spray combustor [20] in the Gas Dynamics and Propulsion Laboratory at the University of Cincinnati, and a preliminary account was presented at Aerospace Sciences meeting in 2005.[14] The inlet air is pre-heated for inlet temperatures up to 1400C at an air mass flow rate up to 1700 slm (2.2kg/minute) with a 36kW electric heater. This inlet flow is conditioned with a series of five fine screens and a honeycomb flow straightener. A triple annular swirler (TAS) with a 5 cm diameter is centered at the dump plane and is installed on the end flange of the plenum chamber. The combustor was operated on a variety of hydrocarbon fuels, and results are presented here for gaseous propane and liquid ethanol.

Two tubular combustion chambers were used: (1) a rectangular chamber with 100x100mm cross-section and 450 mm long with flat quartz windows for optical access, and (2) a round (100 mm diameter) quartz tube 470 mm long with optical access directly through the chamber walls. Exhaust gas is sampled at the combustor exit and analyzed through individual commercial gas analyzers for CO, NOx, and UHC. Both the air- and fuel-flow rates are metered, and other operating parameters, including plenum pressure, inlet air temperature, fuel temperature, combustion flame temperature, and emission data are continuously recorded by a Labview® control program. Two loudspeakers were installed on the plenum chamber and can be driven by a function generator to artificially generate acoustic disturbance for the air flow.

A. Direct absorption temperature sensor near 1.8μm

Figure 4 illustrates the general arrangement used for the 1.8 μm sensor. The output from the DFB laser near 1.8 μm is directed across the flame on the swirl-stabilized spray combustor using appropriate mirrors. The low power (<1mW) 1.8 μm NIR laser is coaligned with a visible laser (HeNe) beam to aid alignment. The diode laser is temperature and current controlled (ILX Lightwave LDC-3900) and injection current tuned over the wavelength region illustrated in Fig. 3. The beam path is purged to avoid interference from ambient water vapor. The laser beam is angled ~10° in the rectangular duct (horizontally) to avoid the etalon interferences from multiple reflections from the flat quartz windows. The total path length is 102 mm.

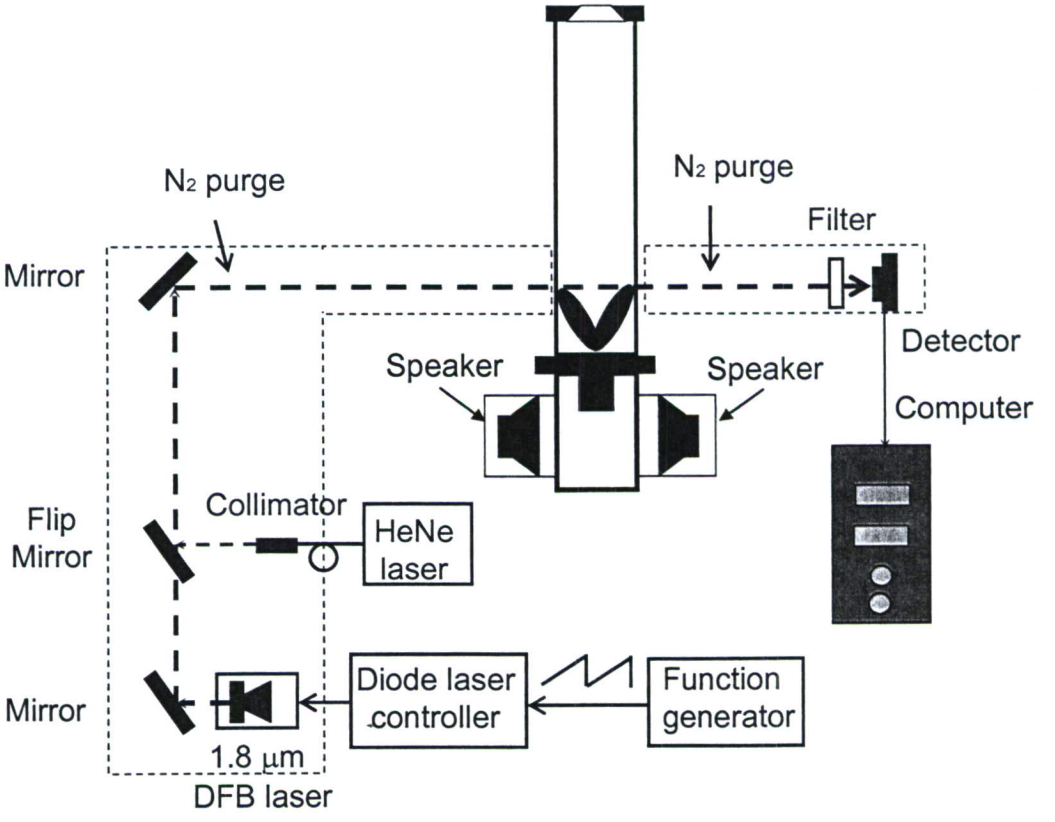

Fig. 4. Schematic diagram of the 1.8 μm temperature sensor applied to the swirl-stabilized spray combustor.

The laser is scanned at 2 kHz and the transmitted intensity is sampled at 1MHz; an average of four scans is used to improve SNR, which reduces the time resolution to 500 Hz. The baseline laser intensity is determined from a polynomial fit to the transmitted intensity beyond the wings of the absorption features, and the absorbance is fit to a convolution of four Voigt absorption lineshapes. Temperature is determined from the ratio of the integrated absorbance of lines 1 and 2 (Table 1) for a single axial location at 50 mm downstream of the nozzle. Fig. 5 shows an example of the absorbance for gas-fueled (0.02kg/minute propane/0.37kg/minute air) and liquid-fueled (0.1kg/min ethanol/2.1kg/minute air) flames. Note the SNR is reduced in liquid-fueled experiments due to beamsteering effects and unburned liquid droplet interference.

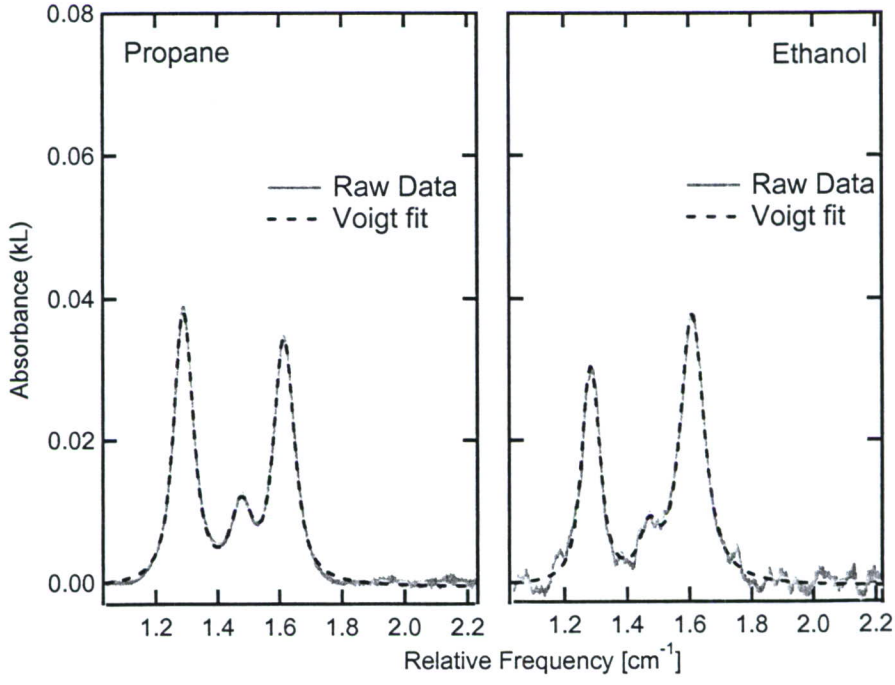

Fig. 5. Direct absorption measurements of H_2O vapor absorption with the 1.8 μm temperature sensor (average of four 2kHz scans) recorded in swirl-stabilized flames with gaseous fuel (propane) and liquid fuel (ethanol).

The airflow can be modulated by driving the plenum pressure with the loudspeakers illustrated in Fig. 4, producing a fluctuating flame stoichiometry (hence heat release rate). Fourier analysis of the time-resolved temperature identifies the fluctuation frequency, illustrating the potential of this sensor for fluctuation measurements. The TDL sensor has line-of-sight (LOS) spatial resolution, and the optimum position to observe these fluctuations is near the flame tip, off the centerline of the burner.

B. Scanned WMS-2f temperature sensor near 1.4 μm

The WMS-2f temperature sensor is illustrated in Fig. 6; the laser beam exits the optical fiber and is collimated with a lens across the flame, filtered and detected. The wavelength of a single DFB diode laser operating near 1.4 μm is injection-current scanned with a 2 kHz sawtooth ramp with a sinusoidal modulation at 500 kHz. The second-harmonic component of the signal from the transmitted laser intensity is isolated by a lock-in amplifier (Perkin-Elmer Model 7280) with a 1 μs time constant. The temperature is inferred from the 2f peak height ratio, with a real-time data processing code written in C++ on a dedicated industrial PC.

The flame is confined in a round quartz duct, and the laser beam is intentionally kept away from the centerline of the round quartz duct to minimize etalon interference. Measurements were made at a radial position 15 mm from the spray centerline and an axial position 50.8 mm downstream of the nozzle exit with a total path length of 97 mm. Figure 7 illustrates representative WMS-2f single scan lineshapes over the wavelength range illustrated in Fig. 3 for gas-fueled (0.08kg/minute propane/ 1.1kg/minute air) and liquid-fueled (0.15 kg/min ethanol/2.1kg/minute air) flames. Note that the SNR is nearly

the same for liquid and gas fuels, illustrating the use of WMS to suppress the low-frequency noise that reduced the SNR of the direct absorption sensor in liquid-fueled flames.

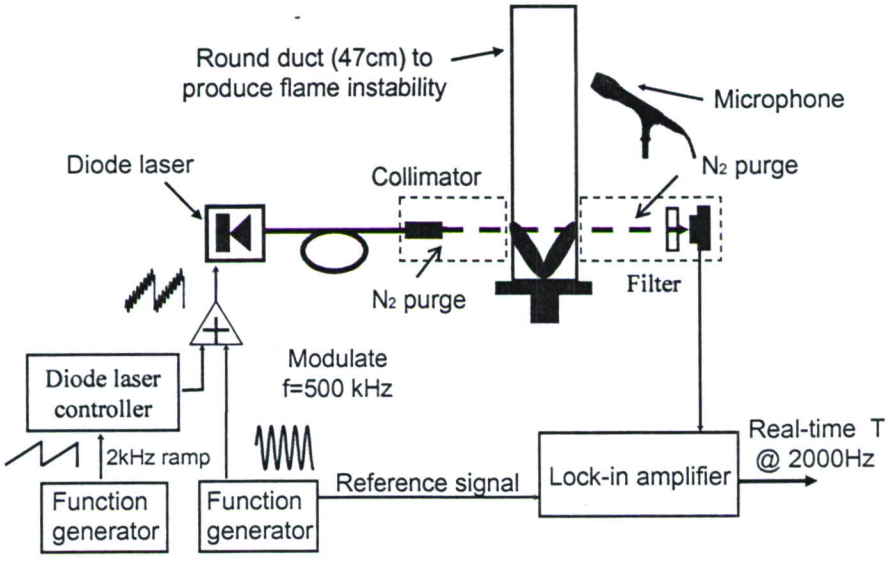

Fig. 6 Schematic diagram of the 1.4 μm temperature sensor applied to the swirl-stabilized spray combustor.

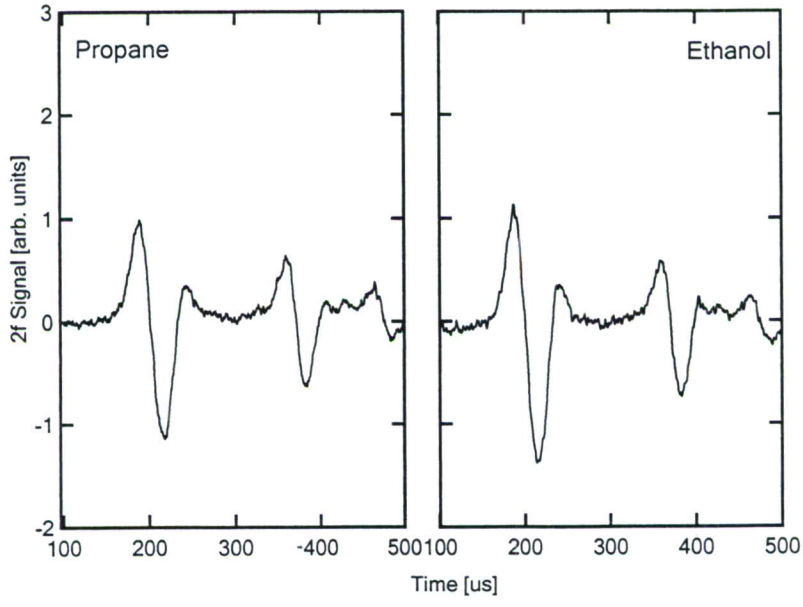

Fig. 7. Scanned WMS-2f H_2O 2f absorption (single scan @ 2kHz) recorded with the 1.4 μm temperature sensor in swirl-stabilized flames with gaseous fuel (propane) and liquid fuel (ethanol).

Figure 8 shows a half second of time-resolved gas temperature data in the propane/air flame. Fourier analysis of these data, also shown, identifies the natural flame instability of the swirl-flame confined in a round duct. The 2kHz scan rate provides a time resolution of 0.5 ms and the temperature analysis provides real-time temperature with this resolution as well as a running FFT (using 0.5 seconds of temperature data). The

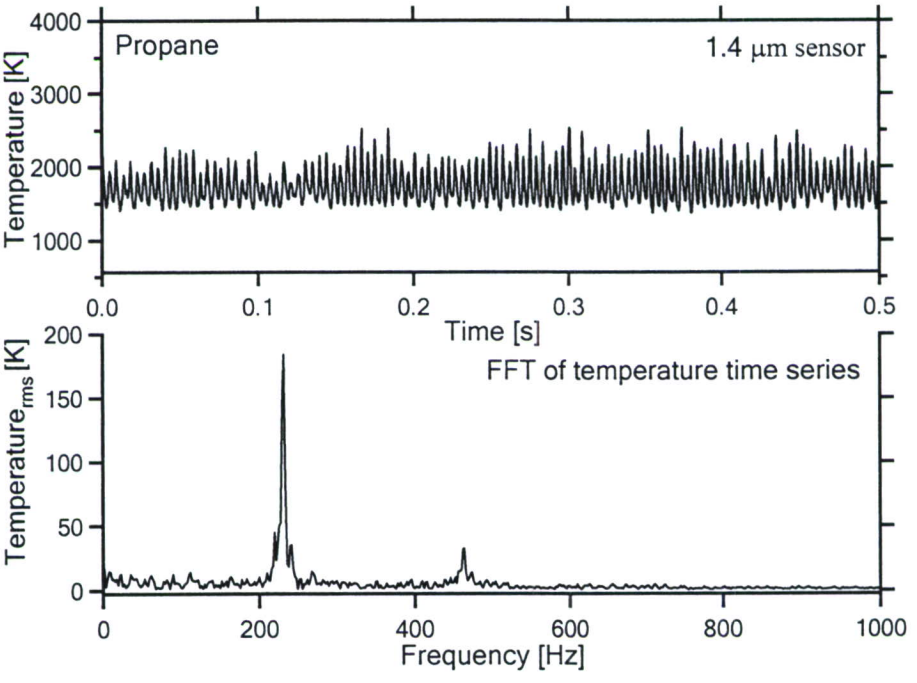

Fig. 8. Measured temperature and its power spectrum in the burned region above the propane-air flame.

dominant mode (232 Hz) and its first harmonic (464 Hz) are clearly revealed. Acoustic signals are simultaneously detected by a Brüel & Kjær microphone (Model 4939-A-011) located 0.5 m from the combustor chamber, and the acoustic signal and its power spectrum shown in Fig. 9 have similar SNR for this flame. These results demonstrate the sensor's ability to track the temperature fluctuations, illustrating a potential application for combustion instability control.

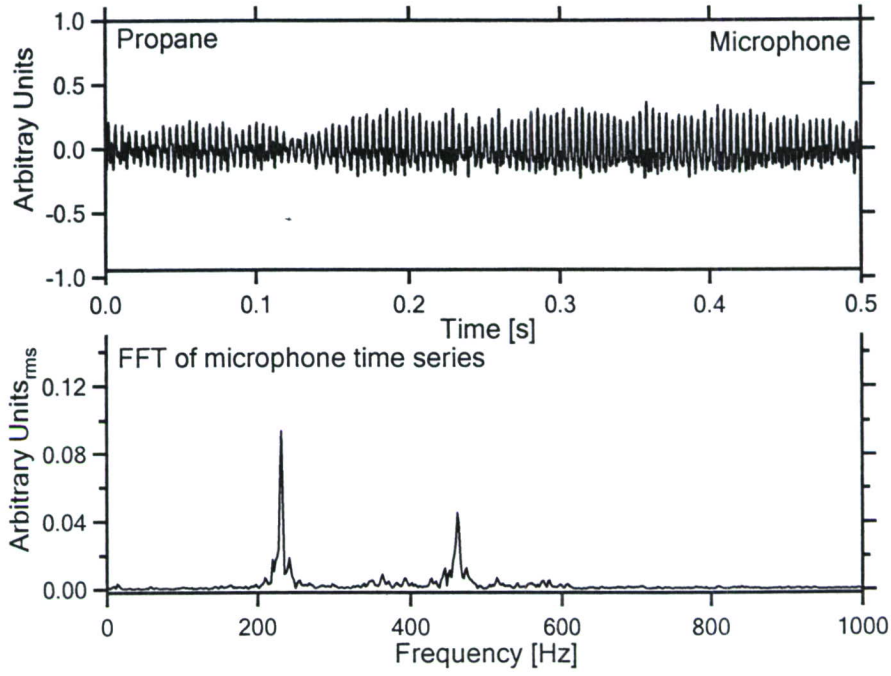

Fig. 9. Measured acoustic signal and its power spectrum in the burned region above the propane-air flame.

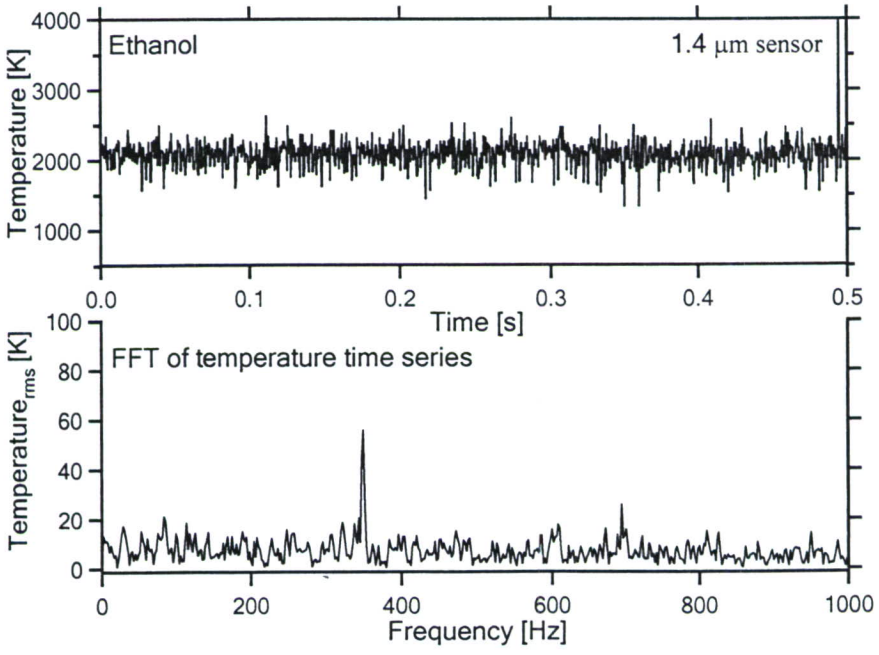

Fig. 10. Measured temperature and its power spectrum in the burned region above the ethanol-air flame.

Similar temperature measurements were made in the ethanol-air flame, as shown in Fig. 10. Here a slightly different duct is used and the dominant 350 Hz mode and its 700 Hz harmonic are clearly evident. Simultaneous microphone measurements are shown in Fig. 11. Although this microphone data has higher SNR, the time limitations of this field measurement campaign did not allow us to optimize the TDL sensor for a quantitative comparison of the two sensors. For example, the TDL LOS was not varied nor did we explore additional filters to reduce the background optical noise on the signal to the lock-in from the more robust liquid-fueled flame.

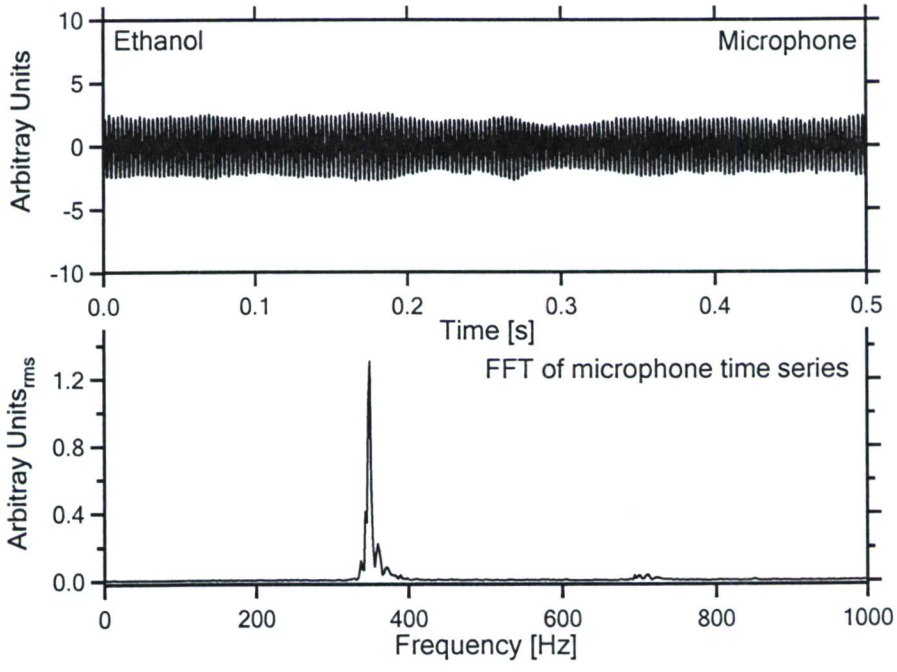

Fig. 11. Measured acoustic signal and its power spectrum in the burned region above the ethanol-air flame.

IV. Discussion of Results from Two TDL Temperature Sensors

To our knowledge, we performed the first TDL thermometry in a liquid-fueled swirl-stabilized spray combustor with support from this project. The TDL sensor is appealing for control applications since it is noninvasive, and has a LOS spatial resolution. The TDL capability to monitor the local temperature fluctuations (hence heat-release fluctuations) provides interesting impetus for investigation of this a temperature sensing for a physics-based control variable. Note that a precision temperature requires a uniform temperature distribution along the sensor LOS. In the practical flames studied here, even though the temperature distribution is not uniform (and thus the sensor does not return a precise temperature), the temporal fluctuations of the temperature provide a useful measure of the flame stability. Subsequent work in our laboratory has shown that these fluctuations provide a very useful control variable for flame stability and to suppress lean blow-out.[21,22]

Although the direct absorption 1.8 μm sensor has the capability to measure temperature of both the gas- and liquid-fueled swirling flames, several limitations are encountered. First, extra efforts are required for the laser alignment and nitrogen purge due to the low power of the laser. Second, the small direct absorption signals required averaging to obtain sufficient SNR under noisy conditions, which limits the measurement bandwidth. Third, the lack of fiber-coupled diode lasers makes the use of this sensor less convenient. These limitations could all be solved with laser devices at 1.8μm similar to the capabilities of telecommunications grade lasers at 1.4μm. The 1.8mm sensor has two additional drawbacks. First the strong room temperature absorption makes the laser sensitive to cold boundary layers in the flame duct, and second the use of a direct

absorption strategy increases the sensitivity to baseline noise and requires data reduction that is not simply amenable to a realtime bandwidth suitable for control applications.

The scanned WMS-2f 1.4 μm temperature sensor has several advantages over the wavelength-scanned direct absorption 1.8 μm temperature sensor:

1. The transitions chosen near 1.4μm were free from interference from room-temperature ambient humidity.
2. The transitions used for the 1.4μm sensor have larger E" and are thus more sensitive to the hottest parts of the LOS path, improving its sensitivity to fluctuations of the high temperature regions along the LOS.
3. The availability of fiber-coupled lasers at 1.4μm provided a low-cost robust sensor.
4. The use of WMS-2f sensor architecture improved the SNR, especially in liquid-fueled flames and enabled rapid data reduction with hardware lock-in analysis.

It is interesting to speculate about the scaling of this work to larger or smaller combustors. The work here illustrates that an atmospheric pressure combustor with a 10 cm path has sufficient signal strength for successful use of either sensor. The scaling of the WMS-2f 1.4μm sensor to smaller combustors depends primarily on how the noise might scale as we have found WMS-2f detection limits three orders of magnitude smaller than the signals from this experiment. Larger combustors produce larger signals, and for combustors larger than 1m LOS pathlength, one might wish to select other weaker transitions. Given the plethora of water vapor transitions in this region, we expect this not to be a limitation and in measurements using similar techniques have been made over a 13m LOS in coal fired power plants.

V. Monitoring and Suppressing Thermoacoustic Instability

The flame of the swirl-combustor is stabilized by the recirculation zones in the flow field: a central recirculation zone (CRZ) created by the swirl and an outer recirculation zone (ORZ) created by the sudden expansion[21] as illustrated in Fig. 12. The recirculation zones produce a region of low velocity with long residence time that allows the flame to propagate into incoming fresh mixture, and serves as a source of continuous ignition for the incoming combustible fuel-air mixture.[22] For stable operation of the flame, most of the chemical reaction occurs between the two hot recirculation zones, and the flame tip is about 5 cm (h/d=1) above the dump surface.

Since the TDL sensor is a LOS measurement, it is important to optimize the positioning of the laser beam. To investigate the effect of laser positioning, a 100 Hz oscillation was introduced in the flame by modulating the intake air flow with four loudspeakers attached to the air conditioning chamber (Fig. 4). To optimize the sensor LOS, measurements were conducted at different horizontal and vertical locations in the forced flame with an air flow rate of 14.1 SCFM and propane flow rate of 0.35 SCFM (ϕ=0.58).

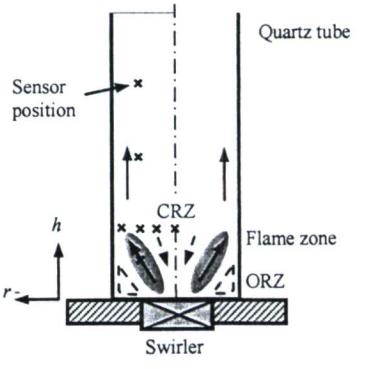

Fig. 12. Schematic of the stable flame structure with central (CRZ) and outer recirculation zone (ORZ) in the flow field. Also indicated are the investigated TDL sensor locations in the flame.

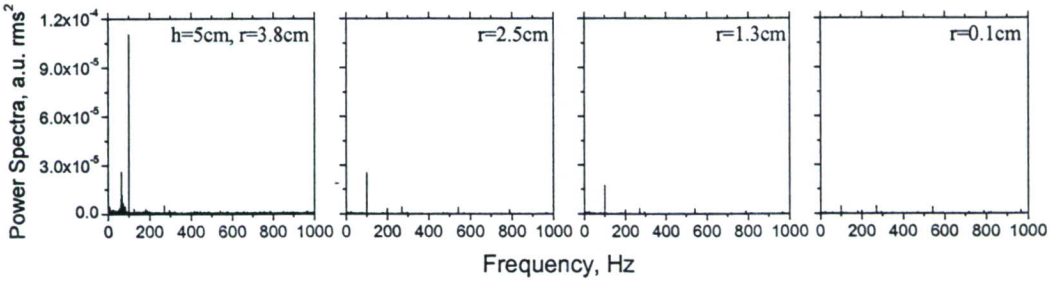

Fig. 13. Measured FFT power spectra of TDL sensor at 4 horizontal locations in the forced flame, h/d=1.

The measured FFT power spectra of the TDL sensor at four horizontal locations (h=d=5 cm) are shown in Fig. 13. At positions very near wall (r/d>0.75), TDL sensor measurements are contaminated by additional low-frequency temperature fluctuations in the boundary layer. At positions near the centerline (r/d=0.02), the TDL sensor poorly identifies the temperature oscillation at 100 Hz, since the gas temperature in the CRZ oscillates at different phase than the oscillation in the flame zone.[23] We find excellent identification of the flame oscillation in the region 0.2<r/d<0.7, and hence we selected the location r/d=0.5 as the best position for the TDL sensor LOS to monitor temperature oscillations.

Similarly we investigated the best vertical position for the TDL sensor LOS. Figure 14 plots the measured FFT power spectra of the TDL sensor at four vertical locations (r=2.5 cm). For sensor positions high in the flame (h/d>2), the signature of the oscillation is nearly buried in the noise because of the mixing of gases from the different regions of the combustor. For h/d<0.5, no flame is observed along the sensor LOS due to the flame structure. For the range 0.5<h/d<1.5, the TDL sensor clearly identifies the flame oscillation. These experiments show that the best region for sensing temperature oscillations is near the flame tip (h/d~1 and r/d~0.5); however, good performance is

observed over a wide range of positions and the sensor LOS does not need to be precisely located.

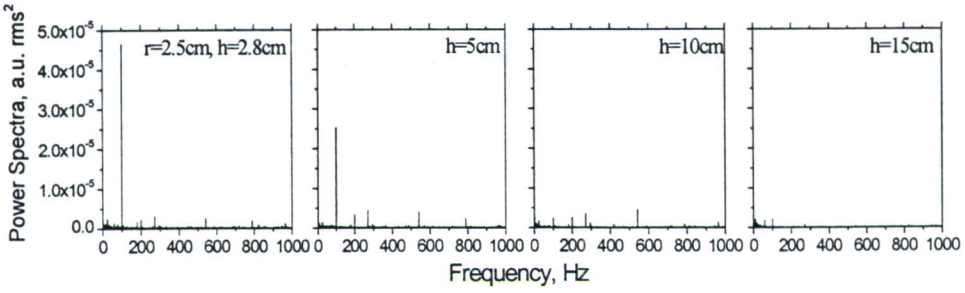

Fig. 14. Measured FFT power spectra of TDL sensor at 4 vertical locations in the forced flame, *r/d*=0.5.

The TDL sensor was also used to monitor the natural thermoacoustic instability induced by the round quartz duct. Figure 15a shows the measured temperature and its FFT power spectrum for a laser LOS near the flame tip with an air flow rate of 29.0 SCFM and propane flow rate of 1.4 SCFM. A time resolution of 0.5 ms is achieved with a laser scan rate of 2 kHz; and an FFT is performed on 0.5-seconds of temperature data, providing a resolution of 2 Hz. The measured acoustic signal and CH* chemiluminescence are also shown in Fig. 15 for comparison. The dominant oscillation mode (232 Hz) and its harmonic (464 Hz) can be clearly seen from the FFT spectra of three sensors. This confirms the interpretation of the temperature data: thermoacoustic instability is the coupling of unsteady heat release to acoustic oscillations. The TDL sensor has some potential advantages for instability control owing to its spatial resolution and insensitivity to background noise and luminosity.

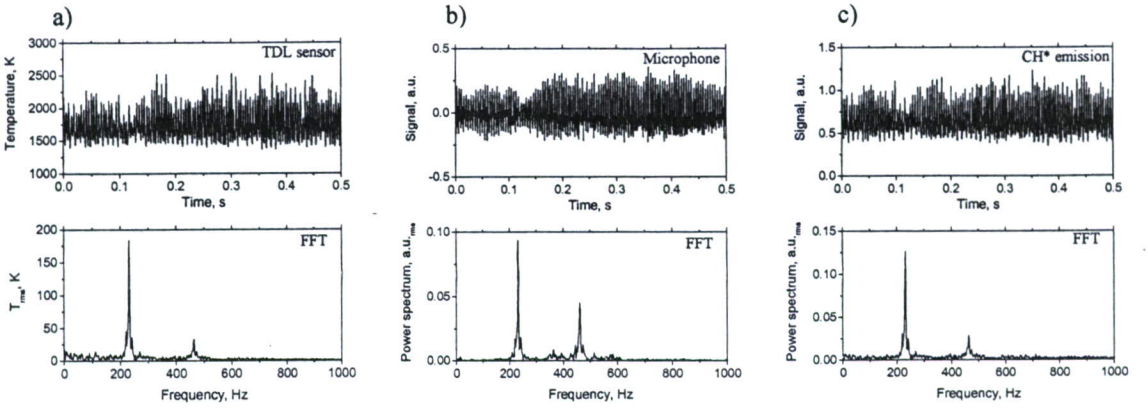

Fig. 15. Measured signals in a propane-air flame with FFT power spectra for: a) TDL sensor; b) microphone; c) CH* chemiluminescence.

Figure 15 illustrates that the TDL sensor can accurately identify flame oscillations and we propose this identification can be developed into a control variable for active suppression of these instabilities. To demonstrate the potential for the use of TDL sensors in combustion control applications, a phase-delay feedback control strategy was investigated in this project, and Fig. 16 illustrates the experiment setup. The 2 kHz real-time sensor output was first time-delayed (dSPACE 1104 board), and this delayed signal was filtered (SR640 low-pass filter and SR645 high-pass filter) and amplified (Phast

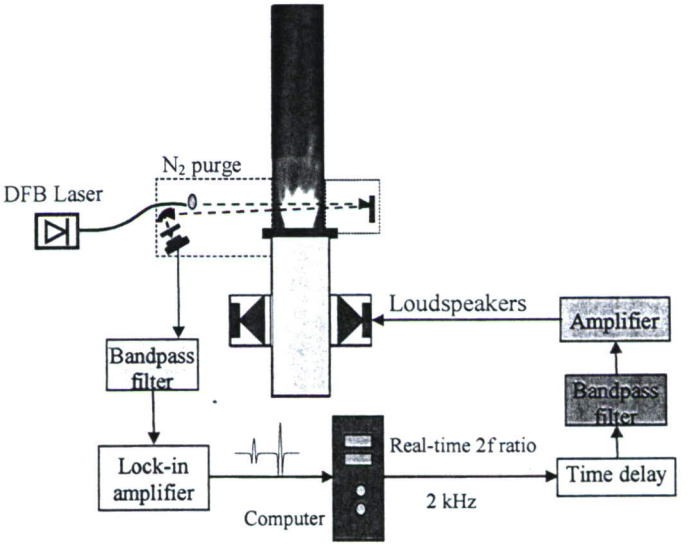

Fig. 16. Experiment setup for phase-delay feedback control.

Landmark, PLB-AMP8) to drive the loudspeakers to modulate the intake air flow. The gain of the feedback system is related to the transfer function of the loudspeaker actuation on the air flow. For this work, the absolute gain was not quantified, as only the relative gain of the amplifier was needed.

Experiments were carried out with a propane flow rate of 1.1 SCFM and air flow rate of 28.1 SCFM. Figure 17 plots the power spectra of the TDL sensor output. Without control, a 388 Hz oscillation is clearly seen in the spectrum (Fig. 9a), whereas with control the thermoacoustic instability is successfully suppressed by the phase-delay feedback control with a time delay of 2 ms and a relative gain of 50.

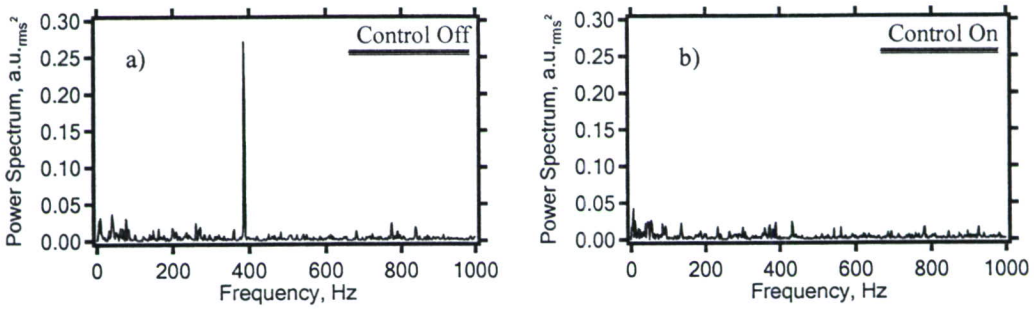

Fig. 17. FFT power spectra of the real-time temperature sensor output for a) control off, and b) control on.

According to Rayleigh criterion, the coupling between the pressure oscillation and the unsteady heat release must be interrupted to suppress combustion oscillations. Experiments were also performed to investigate the effects of phase-delay and relative gain on the active control results. The variation of the temperature oscillations as a function of delay time is shown in Fig. 18a for the instability at 388 Hz (relative gain=50). This controlled behavior is compared with the straight horizontal line that depicts the temperature oscillations when the controller is not operating. Maximum suppression is obtained at a time delay of 2 ms, while maximum destabilization of the

combustion is observed at 0.5 ms, which is approximately at 200° from the optimal phase. At the optimal delay-time, the instability is suppressed by more than 7 dB. The variation of the temperature oscillations as a function of relative gain is also shown in Fig. 18b (delay time=2 ms), and maximum suppression is obtained at a relative gain of 50. These results clearly indicate that the TDL sensor can accurately identify the frequency, phase, and amplitude of the flame instability, and provide the appropriate feedback for the active control system. More advanced control strategies (e.g., adaptive control) and other actuation methods (e.g., secondary fuel injection) are of course possible with this sensor for active control of practical large-scale combustors.

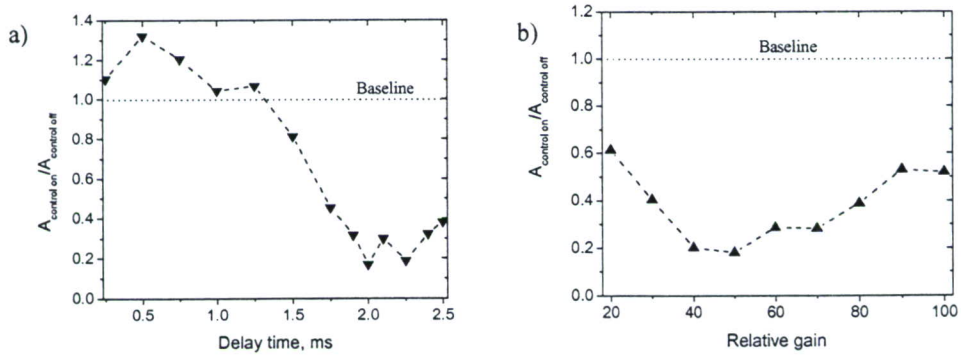

Fig. 18. Amplitude of the temperature oscillations at the instability frequency versus: a) delay time; b) relative gain, for the phase-delay feedback control system.

VI. Application of TDL T-Sensor to Suppress Lean Blow-Out

Photographs of flame are shown in Fig. 19 as the fuel illustrate the change in flame structure as the fuel reduced from stable combustion to an equivalence ratio near LBO for a constant air flow rate. The quenching by flame stretch becomes more important near LBO. There is less heat release between two recirculation zones and more reaction occurs along the wall, resulting in less intense combustion; the flame is less

anchored to the ORZ and becomes unstable. These observations are consistent with the recirculation zone stabilization mechanism of a swirl-stabilized combustor reported by Ref. 21. These flame structures suggest the best location for the sensor LOS for LBO sensing is the shear layer between the CRZ and ORZ or wall (see Fig. 12).

Fig. 19. Flame structure from stable combustion to near LBO

The TDL temperature sensor was used to characterize the flame behavior as equivalence ratio was reduced; the first results were presented in Ref. 25 and 26. In these experiments, the fuel flow rate was decreased gradually, while holding the air flow constant, until LBO occurs. The power spectrum is calculated by a FFT algorithm for every 0.5-second series of recorded WMS-2*f* peak ratio. Figure 20 plots the FFT power spectra of the TDL sensor at two different equivalence ratios: for a stable flame far from blow-out (ϕ-ϕ_{LBO}=0.40) and very near LBO (ϕ-ϕ_{LBO}=0.02) with a sensor location: h/d=1, r/d=0.5. The noise in Fig. 20a is nearly white and typical for steady combustion conditions, whereas the low-frequency fluctuations in Fig. 20b are typical for near-blowout conditions. The data in Fig. 20b illustrate that these low-frequency components increase significantly as the flame approaches LBO, which is consistent with the increase of local extinction/reignition events. There is no characteristic frequency in the power spectrum since the flame extinction events occur randomly. FFT power spectra of the microphone signal and CH* emission at steady combustion and near LBO conditions are

also shown in Fig. 20 for comparison. The microphone data illustrate the noisy flame at steady combustion and the comparatively quiet flame near LBO. The CH* emission signal also diminishes near LBO. These data illustrate the large dynamic range required for LBO detection with the microphone or emission sensors. Thus an advantage of the TDL sensing over the traditional sensors for LBO detection is the large signal on a quiet background for the low-frequency temperature fluctuations.

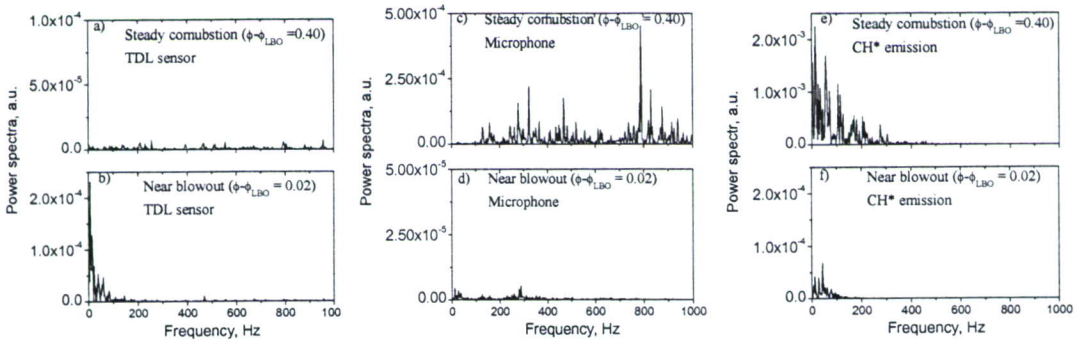

Fig. 20. FFT power spectra of the TDL sensor, microphone, and CH* emission at two different conditions. TDL Sensor location: *h/d*=1, *r/d*=0.5.

The fraction of FFT power in the 0-50 Hz range, $FFT\%_{[0\text{-}50Hz]}$, was used to characterize the low-frequency temperature fluctuations.[24,25] To investigate the effect of laser beam positioning, measurements were conducted at different horizontal and vertical locations in the propane-air flame. Figure 21 shows the measured $FFT\%_{[0\text{-}50Hz]}$ as a function of equivalence ratio at 4 different horizontal locations (air flow rate=25.7 SCFM). It is clear that location r/d=0.5 (across the flame) was the best position for TDL sensor LOS to detect low-frequency temperature fluctuations, which increase sharply as the flame approaches LBO. Approximately 10% of power is in 0-50Hz range when combustion is steady, but this fraction increases to 90% near LBO. At positions very near wall (r/d>0.75), no flame is observed along the sensor LOS due to the flame structure near LBO. At positions near the centerline (r/d=0.02), we find additional low-

frequency temperature fluctuations even for equivalence ratios with stable flames due to the fully reacted gases in the CRZ.

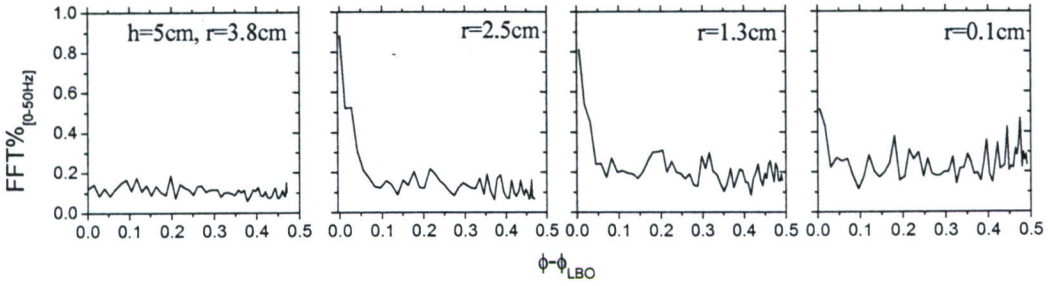

Fig. 21. Fraction of FFT power in 0-50 Hz of the TDL sensor as a function of equivalence ratio at 4 horizontal locations, *h/d*=1. Air flow rate=25.7 SCFM.

Similar experiments were carried out for different vertical locations (*r/d*=0.5), as shown in Fig. 22. The best vertical location for the TDL sensor was at the tip of the flame during stable combustion (*h/d*=1). At positions well above the flame tip (*h/d*>3), additional low-frequency temperature fluctuations were observed even for stable flames due to the effect of gas mixing. At positions very low in the flame (*h/d*<0.5), occasionally no flame was observed along the sensor LOS due to the asymmetric flame structure near LBO. Therefore, the most effective location for the TDL sensor for LBO sensing was at the tip of the flame during stable combustion, i.e., *h/d*~1 and r/*d*~0.5 for current combustor configuration, which was similar to the optimum position found for

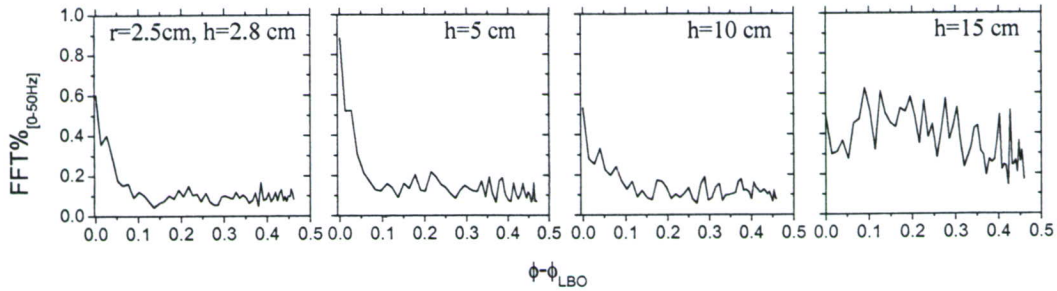

Fig. 22. Fraction of FFT power in 0-50 Hz of the TDL sensor as a function of equivalence ratio at 4 vertical locations, *r/d*=0.5. Air flow rate=25.7 SCFM.

thermoacoustic instability detection. Good LBO sensing was observed at a wide range of positions ($0.5<h/d<2$, $0.25<r/d<0.6$) and the sensor did not need to be precisely located.

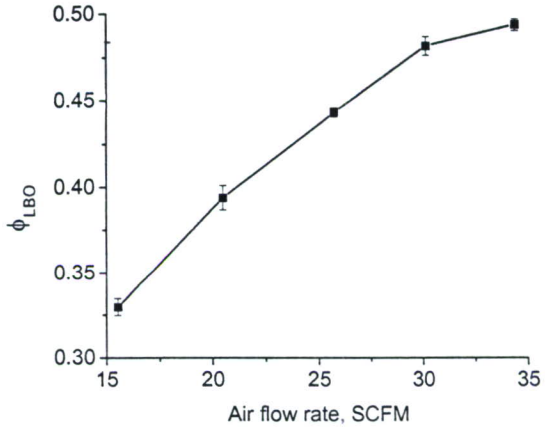

Fig. 23. LBO equivalence ratio as a function of air flow rate.

Similar behavior was observed at various air flow rates from 15 to 35 SCFM. For a specific air flow, the LBO stoichiometry is observed to be repeatable within 0.01; and the LBO limit increases with air flow rate (from 0.33 to 0.49 for the tested air flows), as illustrated by Fig. 23.

The measured increase in low-frequency temperature fluctuations can be used to detect the proximity to LBO without knowing the actual LBO limit for a specific operating condition. Figure 24a plots the measured $FFT\%_{[0\text{-}50Hz]}$ as a function of equivalence ratio and the best fit to the exponential control model[24,25]:

$$FFT\%_{[0-50Hz]} = \frac{T_{rms^2[0,50]}}{T_{rms^2[0,1000]}} = 0.75\exp\left[-(\phi-\phi_{LBO})/0.03\right]+0.12 \qquad (7)$$

A threshold value for $FFT\%_{[0\text{-}50Hz]}$ which is larger than all values of $T_{rms^2[0,50]}/T_{rms^2[0,1000]}$ for steady combustion can be set to distinguish near-blowout conditions from steady conditions[24,25]. There is a range of equivalence ratios near LBO where the flame exhibits

the low-frequency fluctuations shown in Fig. 20 before the fuel is reduced to create an LBO event. This range of equivalence ratios for flames near LBO (ϕ-ϕ_{LBO}<0.05) was successfully identified by the TDL sensor (Fig. 24a), and existed for all conditions studied. For this combustor, we found that the same threshold (FFT%$_{[0\text{-}50Hz]}$=0.25) was suitable to detect LBO for all air flow rates.

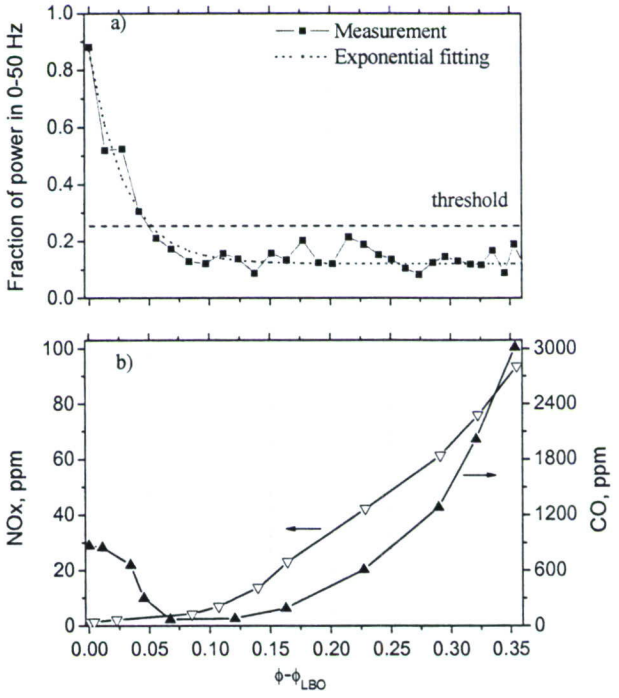

Fig. 24. a) Fraction of FFT power in 0-50 Hz of the TDL sensor output; b) extractive sampling of CO and NOx concentrations (dry-based) in the exhaust gas as a function of equivalence ratio for an air flow rate=25.7 SCFM.

The CO and NOx concentrations measured in the exhaust gas by extractive sampling were consistent with the LBO sensing with TDL sensor, as shown in Fig. 24b. The NOx concentration decreases as equivalence ratio was reduced, mainly due to lower combustion temperature, and a minimum NOx concentration (as low as 1 ppm) was observed near LBO. The CO concentration decreases as equivalence ratio was reduced

while the flame was stable, but the CO concentration increases in the range of equivalence ratios where the flame is unsteady near ϕ-ϕ_{LBO}=0.05. Local extinction and reignition events in this range of unsteady flames near LBO lead to reduced combustion efficiency and increased CO concentration. Therefore, for the current combustor, the optimum operating condition for ultra-lean, low-emission combustion is ϕ-ϕ_{LBO}~0.05. Since the LBO limit, ϕ_{LBO}, depends on flow rates as well as other operating parameters, an active control system will be required to achieve this optimum operation. The TDL sensor can be used to detect the proximity to LBO and the fraction of the noise power at low frequencies was found to be a good control variable ($FFT\%_{[0\text{-}50Hz]}$) for the active suppression of LBO. Active feedback control was demonstrated in our combustor to prevent LBO with a very narrow LBO margin, and thus reduced pollutant emissions[24,25].

VII. Summary of Technical Accomplishments

Two TDL sensors were developed for non-intrusive gas-temperature measurements and their performance was evaluated in gas- and liquid-fueled swirl-stabilized flames. These results were the first demonstration of TDL thermometry in practical liquid-fueled swirl-stabilized flames. Both sensor designs were based on a single-laser two-line ratio concept, which significantly simplified the sensor hardware. The scanned WMS-2f architecture provided several improvements over the wavelength-scanned direct absorption design, as it enabled a real-time temperature readout rate of 2 kHz and superior performance in environments with low-frequency flow-field noise owing to scattering from liquid droplets and soot particles. A strategy for successful detection of incipient lean blow-out (LBO) was demonstrated using this sensor in propane-fueled swirl-stabilized flames. The strength of the low-frequency fluctuations in the region of equivalence ratios just before an LBO event provided an excellent control variable for the suppression of LBO, and hence combustion control was demonstrated enabling stable flame operation with a reduced fuel-air equivalence ratio.

VIII. References

[1]Hanson, R.K. (invited) and Jeffries, J.B., "Diode Laser Sensors for Ground Testing," AIAA paper 2006-3441, June, 2006.

[2]Furlong, E.R., Baer, D.S., and Hanson, R.K., "Real-Time Adaptive Combustion Control Using Diode-Laser Absorption Sensors," *Proceedings of the Combustion Institute,* Vol. 28, 1998, pp. 103-111.

[3]Ebert, V.; Fernholz, T.; Giesemann, C.; Pitz, H.; Teichert, H.; Wolfrum, J.; Jaritz, H "Simultaneous diode-laser-based *in situ* detection of multiple species and temperature in a gas-fired power plant." *Proceedings of the Combustion Institute*, Vol. 28, 2000, pp. 423-430.

[4]Teichert, H., Fernholz, T., and Ebert, V., "Simultaneous in situ measurement of CO, H_2O, and gas temperatures in a full-sized coal-fired power plant by near-infrared diode lasers," *Applied Optics*, Vol. 42, 2003, pp. 2043-2051.

[5]Sanders, S.T., Baldwin, J.A., Jenkins, T.P., Baer, D.S., and Hanson, R.K., "Diode-Laser Sensor for Monitoring Multiple Combustion Parameters in Pulse Detonation Engines," *Proceedings of the Combustion Institute,* Vol. 28, 2000, pp. 587-593.

[6]Rieker, G.B., Li, H., Liu, X., Liu, J.T.C., Jeffries, J.B., Hanson, R.K., Allen, M.G., Wehe, S.D., Mulhall, P.A., Kindle, H.S., Kakuho, A., Sholes, K.R., Matsuura, T., Takatani, S., "Rapid measurements of temperature and H_2O concentration in IC engines with a spark plug-mounted diode laser sensor," *Proceedings of the Combustion Institute,* Vol. 31, 2007, in press.

[7]Mattison, D.W., Jeffries, J.B., Hanson, R.K., Steeper, R.R., DeZilwa, S., Dec, J.E., Sjoberg, M. and Hwang, W., "In-cylinder gas temperature and water concentration measurements in HCCI engines using a multiplexed-wavelength diode-laser system: sensor development and initial demonstration," *Proceedings of the Combustion Institute,* Vol. 31, 2007, in press.

[8]Liu, J.T.C., Rieker, G.B., Jeffries, J.B., Hanson, R.K., Gruber, M.R., Carter, C.D., and Mathur, T., "Near-infrared diode laser absorption diagnostics for temperature and water vapor in a scramjet combustor, *Applied Optics*, Vol. 44, 2005, pp. 6701-6711.

[9]Arroyo, M.P. and Hanson, R.K., "Absorption Measurements of Water Vapor Concentration, Temperature and Lineshape Parameters Using a Tunable InGaAsP Diode Laser," *Applied Optics,* Vol. 32, 1993, pp. 6104-6116.

[10]Gharavi, M. and Buckley, S.G., "Single diode laser sensor for wide-range H_2O temperature measurements."*Applied Spectroscopy*, Vol. 58, 2004, pp. 468-473.

[11]Zhou, X., Liu, X., Jeffries, J.B., and Hanson, R.K., "Development of a Sensor for Temperature and Water Vapor Concentration in Combustion Gases using a Single Tunable Diode Laser," *Measurement Science and Technology,* Vol. 14, 2003, pp. 1459-1468.

[12]Zhou, X., Jeffries, J.B., and Hanson, R.K., "Development of a Fast Temperature Sensor for Combustion Gases using a Tunable Diode Laser," *Applied Physics B.*, Vol. 81, 2005, pp. 711-722.

[13]Zhou, X., Liu, X., Jeffries, J.B., and Hanson, R.K., "Selection of NIR water vapor transitions for in-cylinder measurement of temperature during the compression stroke of an IC-engine," *Measurement Science and Technology*, Vol. 16, 2005, pp. 2437-2445.

[14]Zhou, X., Liu, X., Jeffries, J.B., Hanson, R.K., Li, G., and Gutmark, E.J., "Fast Temperature Sensor for Combustion Control using H_2O Diode Laser Absorption near 1.4 μm," AIAA paper 2005-627, January, 2005.

[15]Reid, J. and Labrie, D., "Second-Harmonic Detection with Tunable Diode Lasers-Comparison of Experiment and Theory," *Applied Physics B*, Vol. 26, 1981, pp. 203-210.

[16]Philippe, L.C. and Hanson, R.K. "Laser Diode Wavelength Modulation Spectroscopy for Simultaneous Measurement of Temperature, Pressure, and Velocity in Shock-Heated Oxygen Flows," *Applied Optics*, Vol. 32, 1993, pp. 6090-6103.

[17]Liu, J.TC., Jeffries, J.B. and Hanson, R.K., "Wavelength Modulation Absorption Spectroscopy with 2f Detection using Multiplexed Diode Lasers for Rapid Temperature Measurements in Gaseous Flows," *Applied Physics B,* Vol. 78, 2004, pp. 503-511.

[18]Hovde, D.C., Hodges, J.T., Scace, G.E. and Silver, J.A., "Wavelength-Modulation Laser Hygrometer for Ultrasensitive Detection of Water Vapor in Semiconductor Gases," *Applied Optics*, Vol. 40, 2001, pp. 829-839.

[19]Rothman, L.S., Barbe, A., Chris Bennerc, D., Brownd, L.R., Camy-Peyrete, C., Carleerf, M.R. *et al.*, "The HITRAN Molecular Spectroscopic Database: Edition of 2000 Including Updates through 2001," *Journal of Quantitative Spectroscopy and Radiative Transfer*, Vol. 82, 2003, pp. 5-44.

[20]Li, G. and Gutmark, E.J. " Combustion Characteristics of a Multiple Swirl Combustor," AIAA paper 2003–0489, January, 2003.

[21]Bradley, D., Gaskell, P.H. Gu, X.J., Lawes, M., and Scott, M.J., "Premixed Turbulent Flame Instability and NO Formation in a Lean-Burn Swirl Burner," *Combustion and Flame*, Vol.115, 1998, pp. 515-538.

[22]Sturgess, G.J., Sloan, D.G., Lesmerises, A.L., Heneghan, S.P., and Ballal D.R., "Design and Development of a Research Combustor for Lean Blow-out Studies," *Journal of Engineering for Gas Turbines and Power,* Vol. 114, 1992, pp. 13-19.

[23]Duan, X.R., Meier W., Weigand, P., and Lehmann, B., "Phase-Resolved Laser Raman Scattering and Laser Doppler Velocimetry Applied to Periodic Instabilities in a Gas Turbine Model Combustor," *Appl. Phys. B*, Vol. 80, 2005, pp. 389-396.

[24]Li, H., Zhou, X., Jeffries, J.B., and Hanson, R.K., "Active Control of Lean Blowout in a Swirl-Stabilized Combustor Using a Tunable Diode Laser," *Proc. Combust. Inst.*, Vol. 31, 2006, in press.

[25]Li, H., Zhou, X., Jeffries, J.B., Hanson, R.K., "Sensing and control of combustion instabilities in swirl-stabilized combustors using a diode laser," *AIAA Journal*, 2006 in press.

PUBLICATIONS AND PRESENTATIONS

1. R.K. Hanson and J.B. Jeffries, "Advances in Laser-Based Sensors for Propulsion Systems, 24th AIAA Aerodynamic Measurement Technology and Ground Testing Conference, paper 2004-2476, AIAA Washington, D.C., 2004.

2. X. Zhou, X. Liu, J.B. Jeffries, R.K. Hanson, Guoqiang Li, and Ephraim J. Gutmark, "Fast Temperature Sensor for Combustion Control using H_2O Diode Laser Absorption near 1.4 μm," *43rd Aerospace Sciences Meeting*, AIAA 2005-627, 2005.

3. X. Zhou, J.B. Jeffries, R.K. Hanson, Q. Lu, and E.J. Gutmark, "Rapid Measurements of Gas Temperature in a Swirl-Stabilized Flame," *Joint Meeting of US Sections of Combustion Institute*, Philadelphia, PA, March 2005.

4. X. Zhou, J.B. Jeffries, R.K. Hanson, "Development of a Fast Temperature Sensor for Combustion Gases Using a Single Tunable Diode Laser," *Applied Physics B.* **81** (2005) 711-722.

5. Ronald K. Hanson (invited) and Jay B. Jeffries, "Advances in Diode Laser Sensors for Combustion and Propulsion," *Western States Section Meeting of the Combustion Institute*, paper 05-F1, Stanford, CA, October, 2005.

6. Ronald K. Hanson (invited) and Jay B. Jeffries, "Advances in Diode Laser Absorption Sensors for Combustion and Propulsion," in *Laser Applications to Chemical, Security, and Environmental Analysis*, Optical Society of America, Washington, D.C., 2006.

7. H. Li, X. Zhou, J.B. Jeffries, R.K. Hanson, "Sensing and Control of Combustion Instabilities in Swirl-Stabilized Combustors using a Diode Laser," *Joint Propulsion Meeting*, Sacramento, CA, July 2006 AIAA 2006- 4395.

8. R.K. Hanson (invited) and J.B. Jeffries, "Diode Laser Sensors for Ground Testing," *25h AIAA Aerodynamic Measurement Technology and Ground Testing Conference*, paper 2006-3441, AIAA Washington, D.C., 2006.

9. X. Zhou, J.B. Jeffries, R.K. Hanson, G. Li, E.J. Gutmark, "Wavelength-scanned tunable diode laser measurements of temperature in a swirl-stablized model gas turbine combustor," *AIAA Journal*, (2006) in press.

10. H. Li, X. Zhou, J.B. Jeffries, R.K. Hanson, "Sensing and control of combustion instabilities in swirl-stabilized combustors using a diode laser," *AIAA Journal*, (2006) in press.

11. H. Li, X. Zhou, J.B. Jeffries, and R.K. Hanson, "Active control of lean blowout in a swirl-stabilized combustor using a tunable diode laser," *Proc. Combustion Institute* **31** (2007) in press.

12. R.K. Hanson and J.B. Jeffries, "Diode Sensors for Combustion and Propulsion," JANNAF 41st Combustion Subcommittee, 29th Airbreathing Propulsion Subcommittee , 23rd Propulsion Systems Hazards Subcommittee, San Diego, CA, December, 2006.